JOURNAL OF MATERIALS SCIENCE 32 (1997) 2093–2097

Effects of Ni addition on mechanical properties of TiB_2/SiC composites prepared by reactive hot pressing (RHP)

G. J. ZHANG, Z. Z. JIN, X. M. YUE
Advanced Ceramics Institute, China Building Materials Academy, Beijing 100024, People's Republic of China

Effects of Ni addition on the mechanical properties of TiB_2/SiC composites produced by RHP according to the chemical reaction $Si + 2TiH_2 + B_4C \rightarrow 2TiB_2 + SiC + 2H_2\uparrow$ have been investigated. The fracture strength and Vickers hardness reach their highest values at 2 wt% Ni content, but the fracture toughness reaches its lowest value at this Ni content. Suitable Ni content can enhance the boundary strength of the composites and it is supported by SEM observation and residual stress measurement by XRD technique. On the other hand, the results of the residual stress measurement show that the residual machining stresses in the surface layer of the specimens are not constant but change with different directions.

1. Introduction

Titanium diboride (TiB_2) is a promising new material for applications in cutting tools, wear resistant parts, anti-corrosive materials and electrodes for aluminium electrolysis because of its high melting point, hardness, wear and corrosion resistance and good electrical conductivity. Nevertheless, the use of TiB_2 is limited because of its brittleness and low oxidation resistance. The additions of second phase particles, such as ZrO_2 [1, 2]. Ti(C, N) [3, 4] and B_4C [5] have been found to be effective in improving the mechanical properties of TiB_2 ceramics. The addition of SiC to ZrB_2 ceramics can improve their oxidation resistance [6]. Similarly, the oxidation resistance of TiB_2 can be improved when SiC is added.

In general, TiB_2-based composites are produced by directly mixing the second phase powder with TiB_2 powder. In our previous work [7], a TiB_2/SiC composite was prepared by reactive hot pressing (RHP) according to the following chemical reaction:

$$TiH_2 \rightarrow Ti + H_2\uparrow$$

$$Si + 2Ti + B_4C \rightarrow 2TiB_2 + SiC \quad (1)$$

The composition from the above reaction gives a volume content of TiB_2 of 71.11% and SiC of 28.89%. The mixed stoichiometric powders of Si, TiH_2 and B_4C were hot pressed at 2000 °C under 30 MPa for 60 min in an Ar atmosphere and the composite obtained has the phase composition of TiB_2 and β-SiC. The bending strength and fracture toughness of the composite were 332 ± 26 MPa and 8.67 ± 0.52 MPa $m^{1/2}$, respectively. The toughening mechanism of the composite was stress-induced microcracking and because the microcracks in TiB_2 matrix with residual tensile stress were easy to link up, the bending strength was low [7].

For TiB_2 ceramics, Ni was determined to be an effective additive for sintering [8] and will improve the boundary strength of the TiB_2 ceramics. Therefore, the strength of the TiB_2/SiC composites prepared by RHP may be enhanced with Ni addition. The present paper will report the results of Ni addition on the mechanical properties of the TiB_2/SiC composites produced by RHP according to Reaction 1.

2. Experimental procedures

The raw powders were TiH_2 (purity 99.5%, particle size < 45 μm), Si (purity $> 99\%$, particle size < 45 μm), B_4C (purity 99%, particle size 5–8 μm) and Ni (purity $> 99.5\%$, particle size < 0.1 μm). The stoichiometric powders according to Reaction 1 with 0, 1, 2, 5 wt% Ni additions (marked by TS-1, TS-2, TS-3 and TS-4, respectively) were mixed in alcohol with WC–Co balls for 4 h in a nylon pot and then dried. The TiB_2/SiC composites were prepared by RHP at 2000 °C under 30 MPa for 60 min in an Ar atmosphere. The products were electrically discharge-machined into specimens and then ground and polished. The water displacement method was used to test the densities of the composites. Fracture strength was tested by the three-point bending method, the size of the specimen was 3 mm × 4 mm × 36 mm and the crosshead speed was 0.5 mm min^{-1}. Fracture toughness was tested using the single edge notched beam (SENB) method (three-point bending); the specimen size was 2 mm × 4 mm × 20 mm, notch width was less than 0.2 mm and depth was about 1.6 mm and crosshead speed was 0.5 mm min^{-1}. The Vickers hardness was tested with a load of 196 N for 15 s. Each datum was an average of 5–6 values. The microstructures of the composites were observed with the scanning

0022–2461 © *1997 Chapman & Hall*

electron microscope (SEM). The residual stresses in the composites were measured by X-ray diffraction (XRD).

3. Mechanical properties and microstructures of the composites

The relative densities of the composites were all in the range of 99.20 to 99.30% theoretical density (TD). Figs 1 and 2 show the changes of the fracture strength, toughness and Vickers hardness of the composites with Ni content. It can be seen that the strength and hardness reach their maximum values at 2 wt % Ni addition; they are 496 MPa and 23.6 GPa, respectively. However, the toughness reaches its minimum value of 6.60 MPa $m^{1/2}$ at 2 wt % Ni addition. It was pointed out that the higher value (8.67 MPa $m^{1/2}$) of fracture toughness with no Ni addition was attributed to the stress-induced microcracking [7]. With the addition of Ni, the boundary strength of TiB_2 phase will be improved and the energy of boundary microcracking will become higher than that of the composite with no Ni addition, so the stress-induced microcracking will be inhibited and the main toughening machanism will be changed. At the same time, the improvement of the boundary strength will enhance the fracture strength and Vickers hardness of the composites. However, additional Ni content greater than 2 wt % Ni will decrease the strength and hardness. This decrease is suggested to be the result of a reaction between TiB_2 and Ni to form TiB [9]. The slight increase in fracture toughness when Ni content was increased from 2 to 5 wt % may be the consequence of the ductile phase toughening by Ni.

The SEM photographs of the polished surfaces of the composites with 0 and 2 wt % Ni additions (TS-1 and TS-3) are shown in Fig. 3. It can be seen that for TS-1, there are many pits on the polished surface which are the result of TiB_2 particles detached from the surface by machining [7], but for TS-3, there are no such pits on the polished surface. This represents an improvement of boundary strength by the Ni addition as mentioned above.

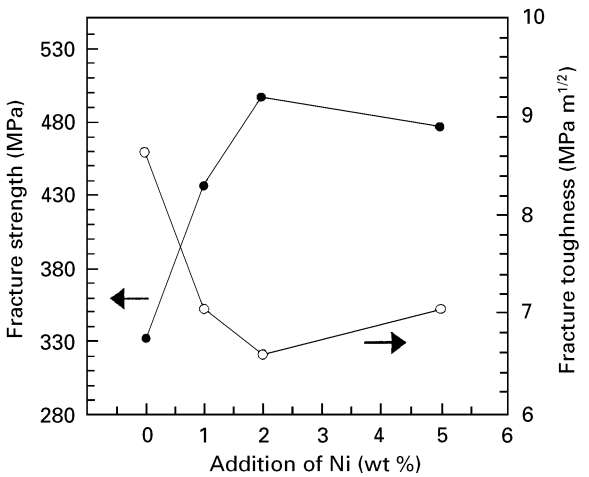

Figure 1 Relationships between σ_f or K_{IC} and levels of Ni addition for the RHPed TiB_2/SiC composites

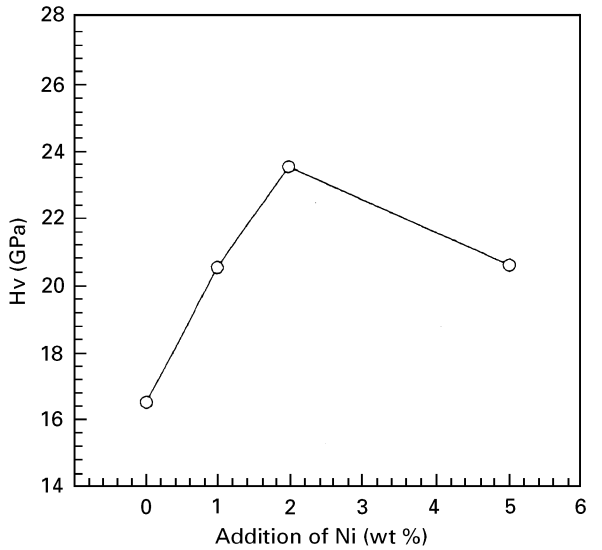

Figure 2 Relationship between Vickers hardness, Hv, and Ni content for the composites

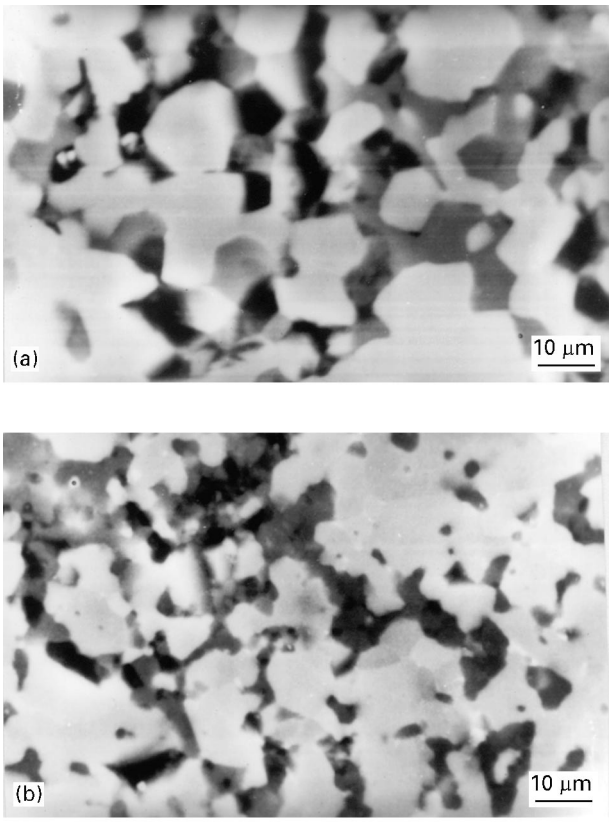

Figure 3 SEM photographs of the polished surfaces of the composites; (a) TS-1 (no Ni addition) and (b) TS-3(2 wt % Ni).

4. Residual stress analysis

According to the calculus proposed by Taya *et al.* [10], the average residual stresses in the TiB_2 matrix and SiC particle induced by the mismatch of the linear thermal expansion coefficients (α) in them are $\langle\sigma\rangle_{TiB_2} = +529$ MPa and $\langle\sigma\rangle_{SiC} = -1302$ MPa (the following data [11] were used in the calculation: $\alpha_{TiB_2} = 8.1 \times 10^{-6}\,°C^{-1}$ and $\alpha_{SiC} = 4.0 \times 10^{-6}\,°C^{-1}$, elastic moduli $E_{TiB_2} = 529$ GPa and $E_{SiC} = 414$ GPa, Poisson's ratio $\nu_{TiB_2} = 0.28$ and $\nu_{SiC} = 0.14$, the

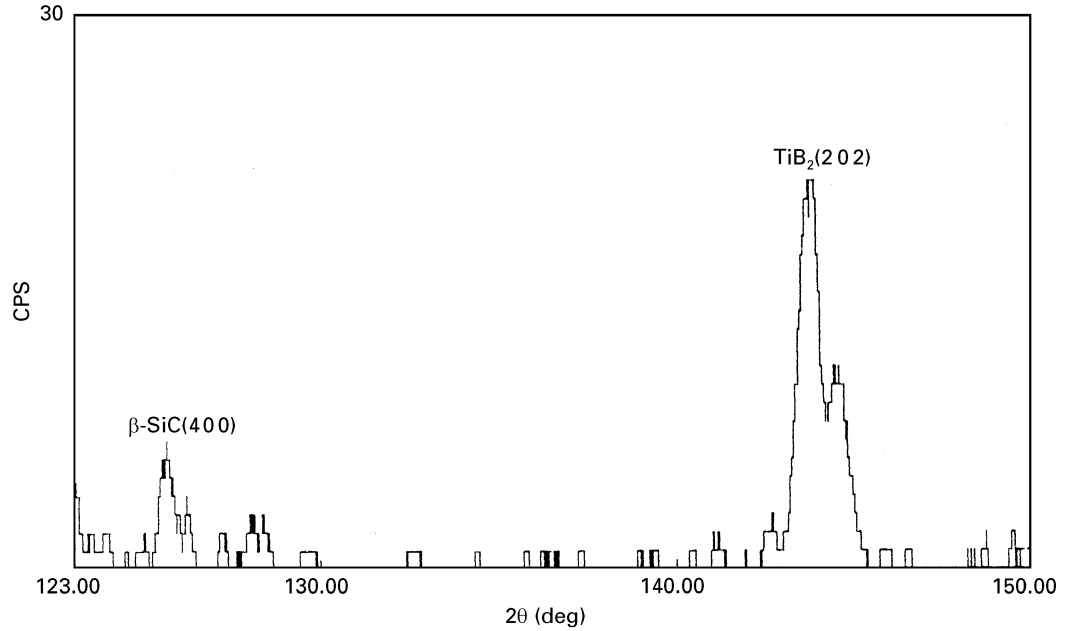

Figure 4 X-ray diffraction intensity peaks used for residual stress measurements.

temperature range over which stresses are not relieved by plastic deformation was set to 1200 K). In the present work, these stresses were measured by X-ray diffraction. The specimens for residual stress measurement were carefully ground. XRD analysis was performed with FeK_α radiation at 40 KeV and 20 mA. The beam size at the sample was approximately $0.5 \times 1.0\,cm^2$. The reflections used were the (2 0 2) ($2\theta = 143.8^\circ$) for TiB_2 and the (4 0 0) ($2\theta = 125.4^\circ$) for β-SiC, as shown in Fig. 4. Fig. 5 shows the coordinate system used for residual stress determination, where S_i are the sample coordinates and L_i are the laboratory coordinates. In this work, we assumed $\sigma_3 = 0$ and ignored the effect of any shear stress. XRD method is based on the measurement of $2\theta_\psi$ at various angles of incident beam tilt φ and ψ as shown in Fig. 5. The stress σ_φ in S_φ direction is the average total stress $\langle {}^t\sigma\rangle_i$ including the residual stress $\langle\sigma\rangle_i$ of each phase caused by thermal expansion mismatch and the residual stress $\langle\sigma^m\rangle$ induced by machining, and can be calculated by [12]:

$$\langle {}^t\sigma\rangle_i = \sigma_\varphi = \frac{-E_i}{2(1+\nu_i)} \operatorname{cotan}\theta_0 \frac{\pi}{180}\left(\frac{\partial(2\theta_\psi)}{\partial(\sin^2\psi)}\right) \quad (2)$$

$$\langle {}^t\sigma\rangle_i = \langle\sigma\rangle_i + \langle\sigma^m\rangle \quad (3)$$

The residual stresses $\langle\sigma\rangle_i$ must sum to zero [13], i.e.

$$\sum f_i\langle\sigma\rangle_i = 0 \quad (4)$$

where i stands for each phase (i.e. TiB_2 and β-SiC), E_i, ν_i are Young's modulus and Poisson's ratio for the i phase, $2\theta_0$ is the diffraction angle of the same peak in the non-stressed sample and it can be replaced by a theoretical datum. $\partial(2\theta_\psi)/\partial(\sin^2\psi)$ is the slope of the line $2\theta_\psi - \sin^2\psi$. f_i is the volume content of the i phase. Solving Equations 3 and 4, one can obtain $\langle\sigma\rangle_{TiB_2}$, $\langle\sigma\rangle_{SiC}$ and $\langle\sigma^m\rangle$. With increasing ψ, the penetration

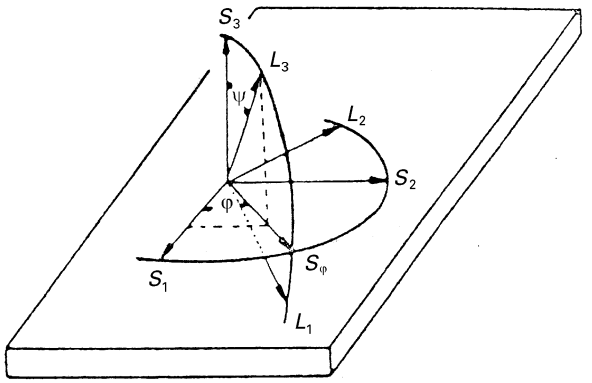

Figure 5 Coordinate system used in residual stress determination: S_i-sample coordinate; L_i-laboratory coordinate.

depth of the X-ray beam into the sample surface will decrease and the fraction of surface residual machining stress will increase, which will affect the linear relationship between $2\theta_\psi$ and $\sin^2\psi$. So the angle ψ should be kept to less than 30°.

Fig. 6 shows the relationship of $2\theta_\psi - \sin^2\psi$ for TiB_2 in TS-1 specimen (the S_φ direction was selected to be vertical to the grinding direction). It can be seen that the values of $2\theta_\psi$ oscillated with the values of $\sin^2\psi$. In general, the height of the XRD peak will be lowered when angle ψ increases, if the specimen has no texture. However, the heights of the peaks for TiB_2 and β-SiC in the composites are also oscillated with angle ψ, sometimes even the shape of the peak was too bad to determine the position of the peak even though angle ψ was small enough. So it is infered that there exists a textural microstructure in the composites which was formed during the RHP process. This phenomenon will affect the measurement of the residual stresses. To simplify this work, only those ψ angles with good peak shapes were used for drawing the $2\theta_\psi - \sin^2\psi$ lines.

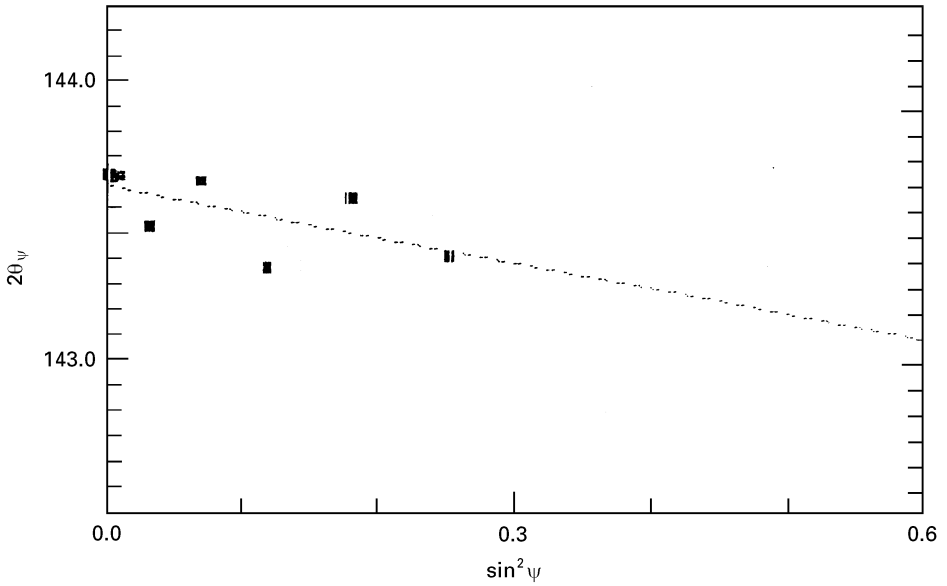

Figure 6 Relationship between $2\theta_\psi$ and $\sin^2\psi$ for TiB_2 in TS-1 specimen, showing oscillation phenomenon.

TABLE I Effect of measurement direction on the result of residual stresses (MPa) for TS-1 sample

S_φ direction	$\langle\sigma\rangle_{TiB_2}$	$\langle\sigma\rangle_{SiC}$	$\langle\sigma^m\rangle$
Vertical to grinding direction	76	− 187	63
Parallel to grinding direction	97	− 240	− 32

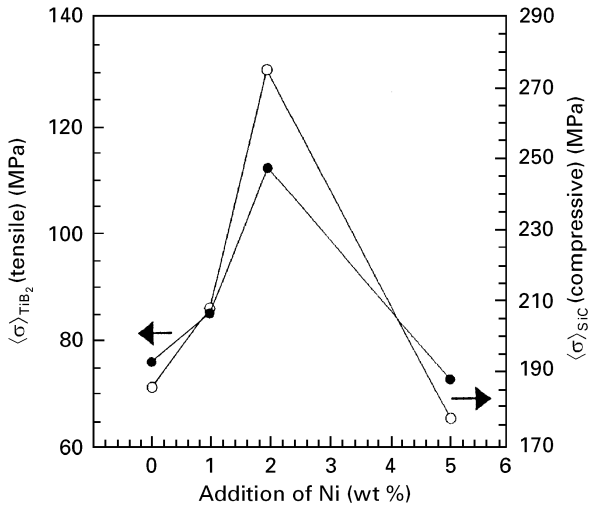

Figure 7 Relationships between the measured residual stresses and the levels of Ni addition for TiB_2 and SiC in the composites.

In order to investigate the effect of grinding direction on the residual stresses induced by grinding and on the measured residual stresses by thermal expansion mismatch, the residual stresses were measured in TS-1 sample when the S_φ direction was vertical and parallel to the grinding direction, respectively, as listed in Table I. It can be seen that in the above two different directions, the residual machining stress was different (compressive in the grinding direction and tensile in the direction vertical to the grinding), which affected the measured values of $\langle\sigma\rangle_{TiB_2}$ and $\langle\sigma\rangle_{SiC}$. So in the following analysis, only the residual stresses measured in the direction vertical to the grinding were used for comparison.

The relationships between the measured residual stresses and the additional Ni content for TiB_2 and SiC are shown in Fig. 7. It can be seen that the residual stresses in TiB_2 and SiC reach their maxima when Ni content is 2 wt %, which coincides with the strength–, fracture toughness– and Vickers hardness–Ni content relationships as shown in Figs 1 and 2. The low residual stresses in TS-1 sample are suggested to be the result of microcracking induced by machining and those for TS-4 sample might be due to the reaction between TiB_2 and Ni with high content. These results support the viewpoint that suitable levels of Ni addition can improve the boundary strength and increase the microcracking energy and inhibit the boundary microcracking induced by applied stress.

5. Conclusions

Effects of Ni addition on the mechanical properties of TiB_2/SiC composites produced by reactive hot pressing are investigated. The bending strength and Vickers hardness have their maxima at a Ni content of 2 wt %, but the fracture toughness reaches its minimum at this Ni content. Suitable levels of Ni addition will improve the boundary strength of the composites, which is supported by SEM observation and residual stress analysis with XRD technique. At the same time, the results of the residual stress measurement show that compressive and tensile residual machining stresses will be induced by grinding in the directions parallel and vertical to the grinding direction, respectively.

Acknowledgement

This work was supported by the National Natural Science Foundation of China (NSFC) on grant no. 59502008.

References

1. T. WATANABE and K. SHOUBU *J. Amer. Ceram. Soc.* **68** (1985) C-34.
2. S. TORIZUKA, K. SATO, J. HARADA, H. YAMAMOTO and H. NISHIO, *J. Ceram. Soc. Jpn.* **100** (1992) 392.
3. K. SHOBU, T. WATANABE and H. YAMAMOTO, *Yogyo-Kyokai Shi* **93** (1985) 46.
4. G. J. ZHANG, *J. Chinese Ceram. Soc.* **21** (1993) 182.
5. T. GRAZIANI, E. LANDI and A. BELLOSI, *J. Mater. Sci. Lett.* **12** (1993) 691.
6. K. SAKAI, *Ceram. Jpn.* **24** (1989) 526.
7. G. J. ZHANG, Z. Z. JIN and X. M. YUE, *Mater. Lett.*, **25** (1995) 97.
8. J. MATSUSHITA, H. NAGASHIMA and H. SAITO, *J. Ceram. Soc. Jpn.* **99** (1991) 78.
9. T. WATANABE and Y. TOKUNAGE, *Bull. Metal Soc. Jpn.* **25** (1986) 1018.
10. M. TAYA, S. HAYASHI, A. S. KOBAYASHI and H. S. YOON, *J. Amer. Ceram. Soc.* **73** (1990) 1382.
11. G. J. ZHANG and Z. Z. JIN, *J. Chinese Ceram. Soc.* **22** (1994) 259.
12. X. FAN (ed.), "X-Ray Technique for Metals" Mechanical Industry Publisher, Beijing, (1981) p. 127.
13. D. J. MAGLEY, R. A. WINHOLTZ and K. T. FABER, *J. Amer. Ceram. Soc.* **73** (1990) 1641.

Received 19 January
and accepted 17 September 1996